AIP | Applied Physics Letters

Evaporation-free inverted organic photovoltaics using a mixture of silver nanoparticle ink formulations for solution-processed top electrodes

Efthymios Georgiou, Achilleas Savva, Marios Neophytou, Felix Hermerschmidt, Tasos Demosthenous, and Stelios A. Choulis

Citation: Applied Physics Letters **105**, 233901 (2014); doi: 10.1063/1.4903893
View online: http://dx.doi.org/10.1063/1.4903893
View Table of Contents: http://scitation.aip.org/content/aip/journal/apl/105/23?ver=pdfcov
Published by the AIP Publishing

Evaporation-free inverted organic photovoltaics using a mixture of silver nanoparticle ink formulations for solution-processed top electrodes

Efthymios Georgiou, Achilleas Savva, Marios Neophytou, Felix Hermerschmidt, Tasos Demosthenous, and Stelios A. Choulis[a)]
Molecular Electronics and Photonics Research Unit, Department of Mechanical Engineering and Materials Science and Engineering, Cyprus University of Technology, 3036 Limassol, Cyprus

(Received 17 September 2014; accepted 30 November 2014; published online 10 December 2014)

We report an investigation of inkjet-printed silver (Ag) nanoparticle inks combined with a poly(3, 4-ethylenedioxythiophene):poly(styrenesulfonate) formulation for solution-processed top electrodes in inverted organic photovoltaics (OPVs) employing the poly(3-hexylthiopehene):phenyl-C61-butyric acid methyl ester material system. We propose a suitable mixture of Ag nanoparticle inks to control the printability and electrical conductivity of the solution-processed top electrode. Based on the proposed solution-processed hole-selective contact, a power conversion efficiency in the range of 3% is reported for evaporation-free inverted OPVs. © *2014 AIP Publishing LLC*.
[http://dx.doi.org/10.1063/1.4903893]

Organic photovoltaic (OPV) devices with prolonged lifetime and printing manufacturing are essential for commercialization prospects of solution-based OPV technologies.[1–4] One of the important research and development OPV milestones is considered to be the avoidance of high vacuum and temperature deposition such as thermal evaporation of the reflective top electrode. Through the use of solution-processed top electrodes, OPVs can be fabricated in a roll-to-roll (R2R) production line[5–7] while simultaneously replacing the energy intensive step of thermal evaporation.

Inverted OPVs could allow more flexibility on designing the R2R production process and thus can provide technological opportunities.[8,9] In addition, inverted OPVs exhibit significantly longer lifetime performance compared to normal structure OPVs, another important parameter for commercialization of such devices.[10–12] However, most of the high performance inverted OPVs reported in the literature use thermally evaporated metal top electrodes.

Recently, efforts have been reported in the literature to eliminate this high energy consuming processing step for the top electrode of inverted OPVs, such as using spray-coated silver nanowires[13] and high-conductivity poly(3,4-ethylenedioxythiophene):poly(styrenesulfonate) (PEDOT:PSS)[14] as well as screen-printed silver inks.[15,16] Furthermore, a relatively thick 800 nm PEDOT:PSS layer has been proposed as hole selective contact suitable for fully solution-processed top electrodes.[16] When the Ag top electrode was inkjet-printed on top of this layer, 2% power conversion efficiency (PCE) was achieved for OPV devices with an active area of 1 cm^2.[16] Very recently, Galagan *et al.* have proposed that a thin layer of a specific formulation of PEDOT:PSS could be robust enough to protect the underlying layers from the diffusion of solvents.[17] This group have achieved 2.8% PCE in devices with 40 nm PEDOT:PSS combined with inkjet printed (IJP) Ag as top electrode with an active area of 0.25 cm^2.

We have recently shown that inkjet printing is a suitable method to print Ag bottom electrodes as a replacement for indium tin oxide (ITO).[18,19] However, in order for an inkjet-printed top electrode to serve as a functional replacement for its evaporated counterpart, it must fulfil two crucial requirements: First, it must wet the underlying PEDOT:PSS layer without dissolving it. Second, the required electrical properties have to be achieved avoiding high temperature sintering, not compatible with the underlying organic active layers.

In this paper, we report an investigation of evaporation-free inverted OPVs with an IJP Ag top electrode. We present functionality and compatibility studies of PEDOT:PSS derivatives combined with a suitable mixture of silver nanoparticle ink formulations in order to achieve the finest printability and the required electrical conductivity of the solution-processed top electrode. Our solution-processed top electrode consists of a double layer (~150 nm) high-conductivity PEDOT:PSS with a suitable IJP Ag ink mixture, providing inverted OPVs with PCE in the range of 3%.

The procedure for the reference device fabrication for the inverted OPVs used in this work is described in detail by Savva *et al.*[20] To ensure good wetting of PEDOT:PSS on top of the hydrophobic poly(3-hexylthiopehene):phenyl-C61-butyric acid methyl ester (P3HT:PCBM) layer, a 0.4% mixture of surfactants (Zonyl and Dynol) in a ratio of 5:2 is added.[20] For the evaporation-free OPV devices, a Dimatix 2800 inkjet printer was employed for Ag ink deposition. The printer parameters were optimized to print a uniform 250 nm Ag layer with a four-device pattern of 9 mm^2 active area. Three silver inks (EMD5603, ANP and a mixture of the two inks) with different solids concentration and nanoparticle sizes were used for this investigation. EMD5603 ink has <150 nm nanoparticle size and 20% solids content dispersed in ethylene glycol. ANP ink has ~50 nm nanoparticle size and 30%–35% solids content dispersed in triethylene glycol monoethyl ether. The third ink is our proposed mixture of 80% EMD5603 Ag ink and 20% ANP Ag ink. For our reference devices with evaporated Ag top electrode, the annealing of the P3HT:PCBM is done at 140 °C for 22 min inside a

a)Email: stelios.choulis@cut.ac.cy

nitrogen-filled glovebox. The annealing of the photoactive layer P3HT:PCBM for the evaporation-free devices was carried out at 140 °C for 20 min before the Ag deposition in a nitrogen-filled glovebox. The sintering temperature of the Ag was set at 140 °C for 2 min on a hotplate in ambient conditions. The J/V characteristics were obtained using a calibrated Newport solar simulator providing an AM1.5G spectrum at 100 mW/cm^2. All the inverted OPVs under study have the following structure ITO/ZnO/P3HT:PCBM/PEDOT:PSS/Ag. Over 50 experimental runs were performed within this study.

Our initial trials to fabricate fully solution-processed electrodes comprised of PEDOT:PSS/IJP Ag nanoparticles, resulted in poor device performance (data are not shown). Diffusion of the inks caused dissolution of the underlying organic layers as previously reported, leading to low electrode selectivity, caused by direct contact of the Ag ink with the semiconducting layer and thus poor inverted OPV performance.[15,16,21,22]

In order to increase the chemical resistance of PEDOT:PSS, we first investigated the effect of increasing the PSS content in PEDOT:PSS hole selective contact.[23] However, our trials did not lead to a significant improvement in evaporation free inverted OPV device performance upon inclusion of this higher PSS content as shown in Figs. 1(b) and 1(c).

Fig. 1(a) demonstrates electrical conductivity measurements performed on all PEDOT:PSS formulations used in this study. The addition of ethylene glycol (EG) in PEDOT:PSS (Clevios PH500) leads to increased electrical conductivity values as described elsewhere.[24] On the other-hand, increasing percentage of PSS content in PEDOT:PSS leads to electrical conductivity decrease for both PEDOT:PSS formulations. Fig. 1(c) indicates the illuminated J/V characteristics of devices with PEDOT:PSS(PH500):ZD:EG(5%) with and without extra PSS(20%). Due to higher conductivity, PEDOT:PSS(PH500):ZD:EG(5%) with and without increased PSS content provides better hole selectivity than PEDOT:PSS PH when combined with Ag printed inks for evaporation-free top electrodes. The addition of PSS content does not eliminate the diffusion issues involved during the processing and sintering procedure, thus resulting in inverted OPVs with poor top electrode selectivity.

A second approach which can be followed to reduce diffusion of Ag ink formulation into the active layer is the deposition of thicker PEDOT:PSS layers.[16] The two aforementioned PEDOT:PSS formulations with different conductivities were used and compared. A 150 nm double layer PEDOT:PSS (for each formulation) was used in combination with IJP EMD5603 Ag ink to form the solution processed top electrode. The J/V characteristics in Fig. 1(d) show

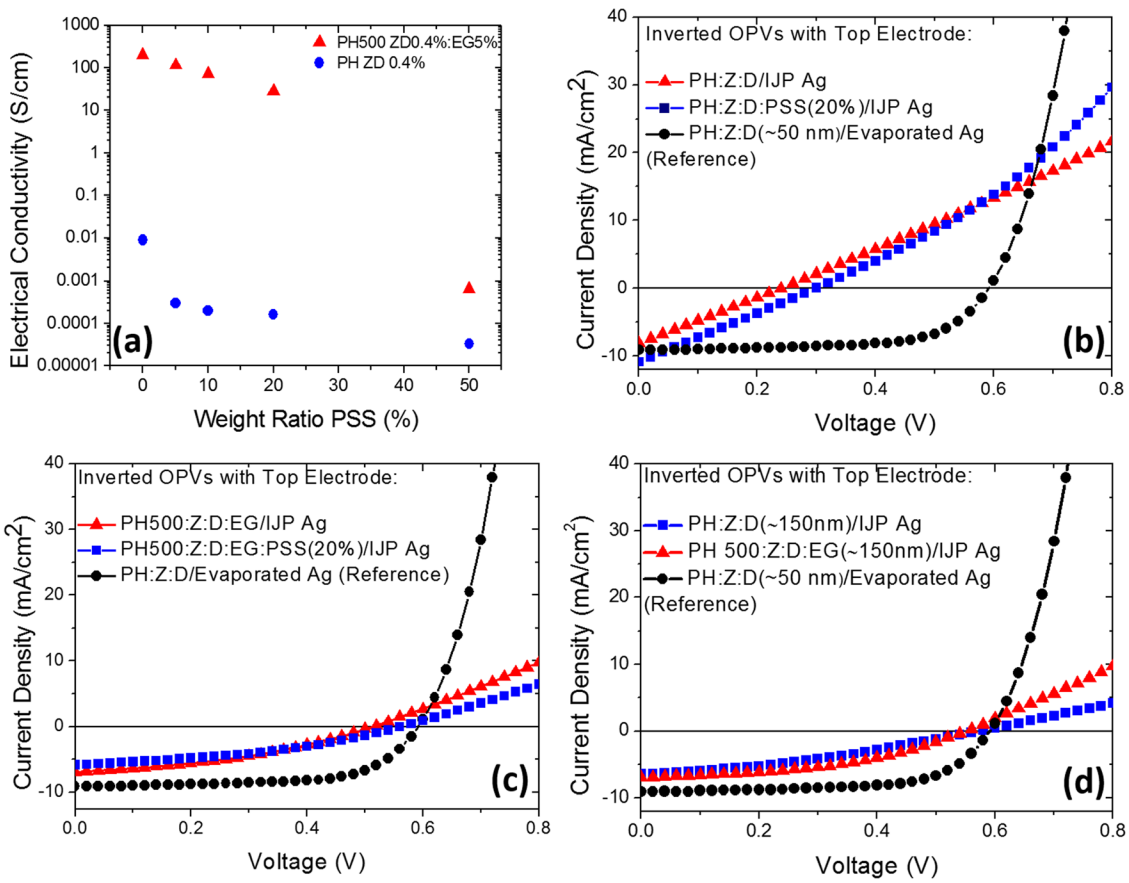

FIG. 1. (a) Conductivity of PEDOT:PSS(PH):ZD and PEDOT:PSS(PH500):ZD:EG as a function of PSS content. (b) Illuminated J/V characteristics of inverted OPVs with top electrode: ~50 nm PEDOT:PSS(PH):ZD with IJP Ag (triangles), ~50 nm PEDOT:PSS(PH):ZD:PSS (20%) with IJP Ag (squares), and ~50 nm PEDOT:PSS(PH):ZD with evaporated Ag (circles). (c) Illuminated J/V characteristics of inverted OPVs with top electrode: ~50 nm PEDOT:PSS(PH500):ZD:EG(5%) with IJP Ag (triangles), ~50 nm PEDOT:PSS(PH500):ZD:EG(5%):PSS(20%) with IJP Ag (squares), and ~50 nm PEDOT:PSS(PH):ZD with evaporated Ag. (d) Illuminated J/V characteristics for inverted OPVs with top electrode: ~150 nm PEDOT:PSS(PH):ZD with IJP Ag (squares), ~150 nm PEDOT:PSS(PH500):ZD:EG with IJP Ag (triangles), and ~50 nm PEDOT:PSS(PH):ZD with evaporated Ag (circles).

that by increasing the thickness of PEDOT:PSS, functional electrodes can be achieved using both PEDOT:PSS derivatives as hole selective contacts. Conductivity issues are critical for solution-processed top electrodes. PEDOT:PSS PH500 with 5% EG has 230 S/cm conductivity as measured with four point probe. This value is approximately five orders of magnitude higher than the conductivity measured for PEDOT:PSS PH (0.01 S/cm). Both approximately 150 nm thick PEDOT:PSS formulations [(PEDOT:PSS(PH):ZD and PEDOT:PSS(PH500):ZD:EG(5%)] resulted in functional evaporation-free inverted OPVs. Fig. 1(d) shows the illuminated J/V characteristics for the devices under study. Based on this study, the PEDOT:PSS (PH500) based formulation provides slightly better fill factor (FF) and series resistance (Rs) values as well as better reproducibility compared to PEDOT:PSS (PH) based formulations for evaporation-free inverted OPVs.

The conductivity limitations also arise due to processing requirements of the IJP Ag nanoparticle top electrodes within the inverted OPV structure. The FF of evaporation-free OPVs is much lower compared to our reference inverted OPVs using low-conductivity PEDOT:PSS (PH) hole selective contact. The reason for the lower FF of the evaporation-free inverted OPVs is due to the low conductivity of the EMD5603 Ag IJP top electrode. The sintering temperature value is limited by the functional properties of the active layer. The sintering has to be carried out at a maximum of 140 °C to avoid negative influence on the performance of P3HT:PCBM active layer. Thus, the conductivity of the particular Ag ink cannot reach higher values as its conductivity is strongly dependent on the optimized OPV processing temperature. Thus, the other critical parameter that can be modified to improve the conductivity values is the metal nanoparticle size. A high sintering temperature provides higher conductivity[19] and a smaller nanoparticle size can provide lower curing temperature. Therefore, ANP inkjet-printed layers are expected to provide higher conductivity at 140 °C due to the smaller nanoparticle sizes they contain.

From a printability point of view, EMD5603 prints well on PEDOT:PSS in contrast with ANP which presents some morphological and patterning issues during the printing and sintering process. During inkjet printing, the ANP ink accumulated in the center of the printed pattern due to its high surface tension and its high solid concentration. During the sintering of ANP ink, a flow from the edges to the center was observed and most of the Ag was accumulated in the center. In order to overcome these problems, ANP was diluted with IPA in a 1:0.5 ratio. Based on this formulation, the inkjet printing parameters of ANP can be improved but not fully resolved (as shown in the J/V characteristics in Fig. 3(a)).

To address the above critical issues, we propose within this paper an ink mixture which can provide solution-based current-collecting electrodes that combine the printability of EMD5603 with the electrical properties of ANP. ANP ink exhibits higher conductivity (35190 S/cm) than EMD5603 (25446 S/cm) ink sintered at 140 °C as measured using the four point probe method. Our optimized ink mixture consisting of 80% EMD5603 and 20% ANP ink demonstrates good printability and slightly higher conductivity values (37713 S/cm) compared with pristine ANP and EMD inks.

In order to examine the surface topography of the Ag inkjet-printed inks, scanning electron microscopy (SEM) and atomic force microscopy (AFM) studies were performed. Fig. 2 shows SEM and AFM images for the three different silver inks sintered at 140 °C for 2 min. Figs. 2(a) and 2(d) represent EMD5603 Ag IJP layers, showing smaller cluster sizes; whereas ANP IJP layers show larger clusters (Figs. 2(b) and 2(e)). Figs. 2(c) and 2(f), then, seem to show both cluster sizes seen for EMD5603 and ANP ink.

As previously reported the Ag cluster size and the agglomeration depend on the sintering temperature and influence the conductivity.[22,25–27] Small nanoparticles have lower curing temperature and thus are able to grow more than the large nanoparticles at 140 °C. The ink mixture contains small (~50 nm) and large (~150 nm) nanoparticle sizes, we suggest that this combination of small and large nanoparticles can form a better network than EMD5603 ink leading also to slightly higher conductivity values compared to the ANP ink. More importantly, the proposed Ag ink mixture eliminates printing processing limitations providing functional top contact and intimate interfaces for the solution processed top electrode.

In order to compare the different ink formulations with the evaporated Ag, the three different ink formulations (EMD5603, ANP and ink mixture) have been inkjet-printed on the reference ~50 nm PEDOT:PSS:ZD layer. Comparing the three evaporation-free inverted OPVs, the best PCE value is achieved using the ink mixture as shown in Fig. 3(a). The inset of Fig. 3(a) shows the magnification of the Rs region.

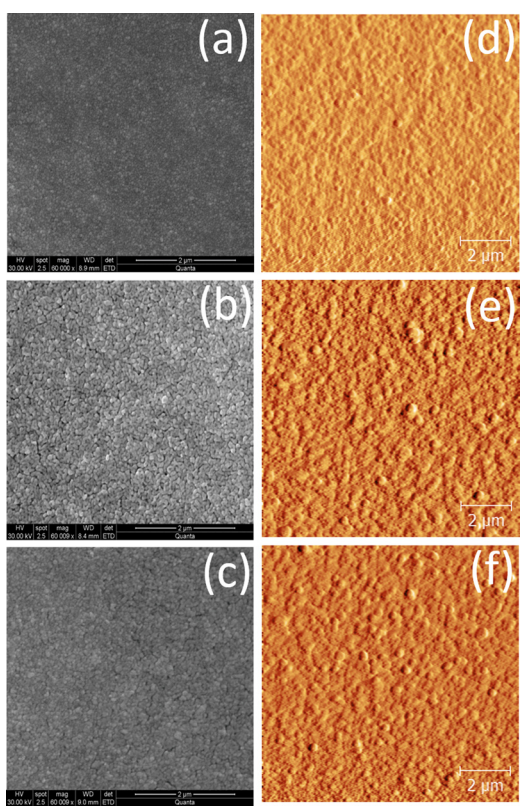

FIG. 2. SEM ((a)–(c)) and AFM ((d)–(f)) images of inkjet-printed EMD5603 Ag ink ((a) and (d)), ANP:IPA (1:0.5) Ag ink ((b) and (e)), and Ag ink mixture ((c) and (f)) on glass. The scale bar for all images is 2 μm.

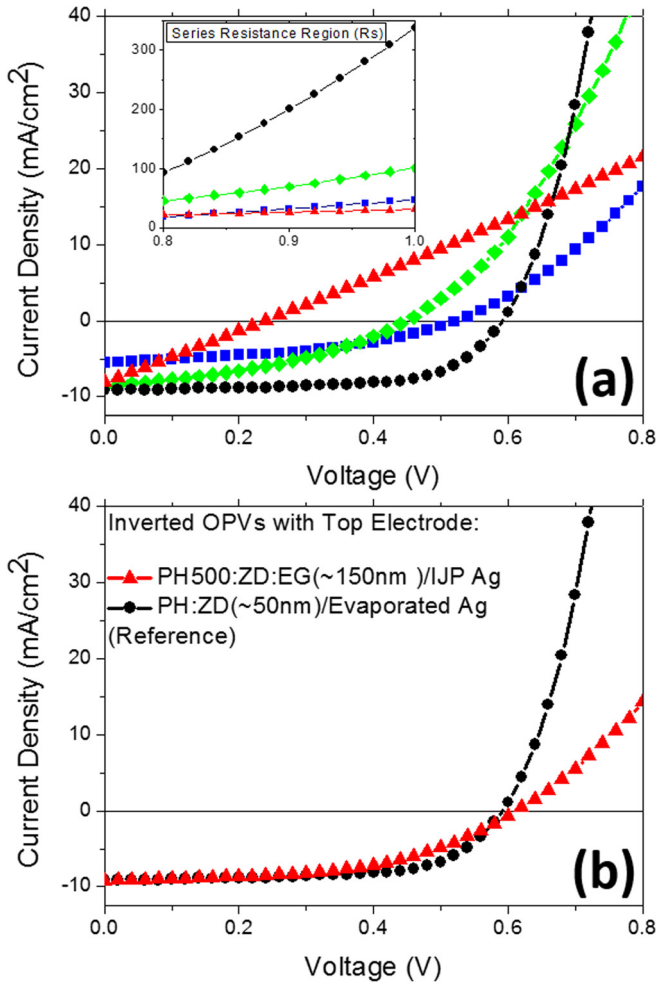

FIG. 3. (a) Illuminated J/V characteristics of inverted OPVs with top electrode PEDOT:PSS(PH):ZD and IJP Ag with EMD5603 ink (red triangles), ANP:IPA (1:0.5) ink (blue squares), mixture ink (green diamonds), and evaporated Ag (black circles). (b) Illuminated J/V characteristics of inverted OPVs with top electrode: ~150 nm PEDOT:PSS(PH500):ZD:EG(5%) and IJP silver mixture (triangles), ~50 nm PEDOT:PSS(PH):ZD with evaporated Ag (circles).

The ink mixture has the highest Rs and the ANP ink has an intermediate value. The EMD5603 ink has the lowest Rs, however this value must be taken with caution as the curve does not show diode-like behavior.

When then combining the previously established 150 nm layer of PEDOT:PSS (PH500):ZD:EG(5%) with the Ag ink mixture, the resulting J/V characteristics are shown in Fig. 3(b) together with our reference inverted OPVs using evaporated silver top electrode and PEDOT:PSS(PH):ZD-(50 nm) hole selective contact. The evaporation-free inverted OPVs containing IJP Ag (ink mixture) top electrodes only show slightly lower PCE compared to our optimized reference inverted OPVs. The PCE parameters such as Voc and Jsc have similar values as shown in Table I. The main drop is observed in the FF which is 65% in our reference inverted OPVs and 51% for the optimum evaporation-free inverted OPVs. Despite the above limitations on the hole carrier selectivity of the proposed solution-processed top electrode for inverted OPV performance, a 2.9% PCE has been achieved for evaporation-free inverted OPVs using the proposed 150 nm and highly conductive PEDOT:PSS formulation

TABLE I. PCE performance parameters of the reference (evaporated Ag) inverted OPVs and our optimum evaporation-free inverted OPVs with IJP Ag.

OPV	Jsc (mA/cm^2)	Voc (V)	FF (%)	PCE (%)
Reference	9.09	0.59	65.16	3.50
IJP	9.21	0.61	51.36	2.89

combined with the proposed IJP Ag ink mixture. We note that PCE reduction is expected for larger than 1 cm^2 active area devices due to a likely increase in series resistance (Rs) as experimentally studied by Kopola *et al.*[6]

In summary, we investigated the fabrication of the solution-processed top electrode in inverted OPV devices. The crucial points which deserve consideration during the fabrication of solution-processed top electrodes are each layer's wetting properties and the prevention of dissolving of the underlying layers. We have shown that electronic properties, printing parameters, and intimate interfaces are critical to achieve high performance solution-processed top electrodes. A double layer of PEDOT:PSS(PH500):ZD:EG(5%) with overall thickness of approximately 150 nm, can provide a functional hole selective contact for solution-processed top electrodes and can be used to partly resolve the limitations caused by diffusion of the Ag ink formulation in PEDOT:PSS. However, there are still many critical challenges that need to be overcome in order to eliminate diffusion issues on the way to achieving high performance solution-processed top electrodes for long lived evaporation-free inverted OPVs.

Importantly, by mixing suitable Ag inks with different nanoparticle sizes and curing temperature, we have shown that adequate conductivity and inkjet printing processing properties at sintering temperatures compatible with the requirements of inverted OPVs solution processed requirements, can be achieved. For all the experimental runs performed in our labs using different PEDOT:PSS hole selective contacts, the ink mixture showed it could be used to improve the PCE of inverted OPVs incorporating solution-processed top electrode. The resulting evaporation-free inverted OPVs reached 2.9% PCE in comparison to our optimized reference inverted OPVs exhibiting PCE of 3.5%.

We would like to acknowledge Cyprus Research Promotion foundation for funding the development of the Molecular Electronics and Photonics Research Unit at Cyprus University of Technology under Research Grant "NEW INFRASTRUCTURE/STRATEGIC/0308/06," and thank Professor A. Anayiotos and K. Kapnisis for their assistance on the SEM measurements.

[1]B. Azzopardi, C. J. M. Emmott, A. Urbina, F. C. Krebs, J. Mutale, and J. Nelson, Energy Environ. Sci. **4**(10), 3741 (2011).
[2]C. J. M. Emmott, A. Urbina, and J. Nelson, Sol. Energy Mater. Sol. Cells **97**, 14 (2012).
[3]F. Machui, M. Hösel, N. Li, G. D. Spyropoulos, T. Ameri, R. R. Søndergaard, M. Jørgensen, A. Scheel, D. Gaiser, K. Kreul, D. Lenssen, M. Legros, N. Lemaitre, M. Vilkman, M. Välimäki, S. Nordman, C. J. Brabec, and F. C. Krebs, Energy Environ. Sci. **7**(9), 2792 (2014).

[4]N. Espinosa, R. García-Valverde, A. Urbina, F. Lenzmann, M. Manceau, D. Angmo, and F. C. Krebs, Sol. Energy Mater. Sol. Cells **97**, 3 (2012).
[5]F. C. Krebs, S. A. Gevorgyan, and J. Alstrup, J. Mater. Chem. **19**(30), 5442 (2009).
[6]P. Kopola, T. Aernouts, R. Sliz, S. Guillerez, M. Ylikunnari, D. Cheyns, M. Välimäki, M. Tuomikoski, J. Hast, G. Jabbour, R. Myllylä, and A. Maaninen, Sol. Energy Mater. Sol. Cells **95**(5), 1344 (2011).
[7]F. C. Krebs, Org. Electron. **10**(5), 761 (2009).
[8]C. Waldauf, M. Morana, P. Denk, P. Schilinsky, K. Coakley, S. A. Choulis, and C. J. Brabec, Appl. Phys. Lett. **89**(23), 233517 (2006).
[9]A. Savva and S. A. Choulis, Appl. Phys. Lett. **102**(23), 233301 (2013).
[10]E. Voroshazi, B. Verreet, A. Buri, R. Muller, D. Di Nuzzo, and P. Heremans, Org. Electron. **12**(5), 736 (2011).
[11]K. Norrman, M. V. Madsen, S. A. Gevorgyan, and F. C. Krebs, J. Am. Chem. Soc. **132**(47), 16883 (2010).
[12]V. M. Drakonakis, A. Savva, M. Kokonou, and S. A. Choulis, Sol. Energy Mater. Sol. Cells **130**, 544 (2014).
[13]J. Krantz, T. Stubhan, M. Richter, S. Spallek, I. Litzov, G. J. Matt, E. Spiecker, and C. J. Brabec, Adv. Funct. Mater. **23**(13), 1711 (2013).
[14]Y. F. Lim, S. Lee, D. J. Herman, M. T. Lloyd, J. E. Anthony, and G. G. Malliaras, Appl. Phys. Lett. **93**(19), 193301 (2008).
[15]F. C. Krebs, R. Søndergaard, and M. Jørgensen, Sol. Energy Mater. Sol. Cells **95**(5), 1348 (2011).
[16]D. Angmo, J. Sweelssen, R. Andriessen, Y. Galagan, and F. C. Krebs, Adv. Energy Mater. **3**(9), 1230 (2013).
[17]Y. Galagan, S. Shanmugam, J. P. Teunissen, T. M. Eggenhuisen, A. F. K. V. Biezemans, T. Van Gijseghem, W. A. Groen, and R. Andriessen, Sol. Energy Mater. Sol. Cells **130**, 163 (2014).
[18]M. Neophytou, F. Hermerschmidt, A. Savva, E. Georgiou, and S. A. Choulis, Appl. Phys. Lett. **101**(19), 193302 (2012).
[19]M. Neophytou, E. Georgiou, M. M. Fyrillas, and S. A. Choulis, Sol. Energy Mater. Sol. Cells **122**(C), 1 (2014).
[20]A. Savva, M. Neophytou, C. Koutsides, K. Kalli, and S. A. Choulis, Org. Electron. **14**(11), 3123 (2013).
[21]Y. Noguchi, T. Sekitani, T. Yokota, and T. Someya, Appl. Phys. Lett. **93**(4), 043303 (2008).
[22]C. Girotto, B. P. Rand, S. Steudel, J. Genoe, and P. Heremans, Org. Electron. **10**(4), 735 (2009).
[23]J. Yang, R. Zhu, Z. Hong, Y. He, A. Kumar, Y. Li, and Y. Yang, Adv. Mater. **23**(30), 3465 (2011).
[24]Z. Hu, J. Zhang, Z. Hao, and Y. Zhao, Sol. Energy Mater. Sol. Cells **95**(10), 2763 (2011).
[25]K. S. Chou, K. C. Huang, and H. H. Lee, Nanotechnology **16**(6), 779 (2005).
[26]K. Park, D. Seo, and J. Lee, Colloids Surf., A **313–314**, 351 (2008).
[27]H. H. Lee, K. S. Chou, and K. C. Huang, Nanotechnology **16**(10), 2436 (2005).